Available online at www.sciencedirect.com
ScienceDirect
Colloids and Surfaces A: Physicochem. Eng. Aspects 292 (2007) 42–50
COLLOIDS AND SURFACES A
www.elsevier.com/locate/colsurfa

Dielectric relaxation spectroscopy of macroporous IER beads suspensions dispersed in primary alcohols and water–ethanol mixtures

Zhen Chen, Kong-Shuang Zhao *

College of Chemistry, Beijing Normal University, Beijing 100875, China

Received 23 March 2006; received in revised form 1 June 2006; accepted 5 June 2006
Available online 10 June 2006

Abstract

Dielectric measurements were first carried out on suspensions of ion-exchange resin beads dispersed in primary alcohols and water–ethanol mixtures in the frequency range 40 Hz–110 MHz. Due to the large bead radius, only Maxwell–Wagner (M–W) dielectric relaxations were observed. Regular dielectric behaviors were observed and phase parameters concerning constituent phases' properties were determined through dielectric analysis, which revealed that the properties and the dispersing state of the bead are strongly dependent on the properties of dispersion medium. It is also found that dry beads cannot be completely soaked by alcohols with long aliphatic chain, and that suspension in water-rich mixture has similar dielectric behavior as in pure water due to the mixture's molecular construction. Then the dielectric behaviors of the following suspensions were measured as a function of time: suspensions of beads that have been equilibrated with water/ethanol redispersed in ethanol/water. The dielectric behaviors showed remarkable time dependency, characterized by distinct transitions on the curves of time dependent relaxation parameters. Based on the above understandings, the time dependent dielectric behaviors were analyzed in detail. It is showed that the time dependency directly reflected such processes as ion diffusion, solvent diffusion and solvent uptake that the systems undergo.

Keywords: Dielectric relaxation spectroscopy; Ion-exchange resin beads; Water–ethanol mixture; Hanai's equation; Concentrated suspension

1. Introduction

Maxwell–Wagner (M–W) polarization [1–3] and counterion polarization (concentration polarization) [4–6] are two most typical polarization mechanisms for particle suspensions subject to an oscillating field. The former is owing to the famous M–W effect [1,2] extended by O'Konski [7] by introducing the concept of surface conductivity, typically occurring at frequency of the order of megahertz. While the latter arises from the diffusion of ions in the bulk solution adjoining the electric double layer (EDL) according to the recent understandings [6,8–12], which may occur at frequency down to a few hertz or up to several kilohertz resting with the size of the dispersed particle. Due to the development of theoretical [8–12] and numerical [13–16] treatment in the last 40 years, dielectric relaxation spectroscopy (DRS) based on these mechanisms has become one of the most practical methods used for the characterization of particle suspensions, offering valuable information about the electrical properties of particle, dispersion medium and their interfaces [17–22].

Despite a number of successful applications, experimental investigations still lag seriously behind theoretical studies. Furthermore, these theories cannot be applied to most actual systems due to their theoretical restrictions, and actual systems usually involve more complicated polarization processes, for example porous materials [23,24]. This situation demands that more experimental investigations on actual systems should be carried out. On the other hand, DRS has some unique advantages: (1) it is rather sensitive to the properties of constituent phases and interfaces, which guarantees that even tiny changes of the system under measurement can be identified; (2) it is non-invasive, making in situ dielectric measurement on the systems in their working state to be possible; and (3) dielectric measurement can be completed very quickly so that non-equilibrium systems can be instantaneously monitored. Therefore, even without theoretical schemes it is still possible to obtain valuable information about actual systems by means of DRS.

* Corresponding author. Tel.: +86 10 58808283.
E-mail address: zhaoks@bnu.edu.cn (K.-S. Zhao).

0927-7757/$ – see front matter © 2006 Elsevier B.V. All rights reserved.
doi:10.1016/j.colsurfa.2006.06.001

Suspensions of macroporous ion-exchange resin (IER) beads were studied through DRS in this work. A number of polarization processes may contribute to the dielectric response of charged porous particle suspensions in a wide frequency range, as shown in the works of Chelidze et al. [17,23,24]. However, in the frequency of the order of megahertz, M–W effect or interfacial polarization dominates. Our previous DRS studies [25,26] on aqueous IER beads suspensions showed that the M–W type dielectric relaxation was mainly decided by counterion association and electromigration on the bead/solution interface. Since these interfacial properties change markedly with the dielectric constant of the dispersion medium [27], and it is hoped that the change may be detected by DRS, we first measured the dielectric behaviors of equilibrium suspensions dispersed in primary alcohols and water–ethanol mixtures. It will show that the dielectric behaviors are close related to the properties of the solvents and the configuration of the bead. Particle suspensions in non-equilibrium state are rarely investigated by DRS. However, non-equilibrium processes in any phase of a suspension will end up with a variation on the interface, therefore these processes are also hoped to be monitored by DRS due to its aforementioned advantages. To this end, on-line dielectric measurements were carried out on the following suspensions: (a) beads that have been equilibrated with water redispersed in ethanol (for the convenience of expression we call it water-equilibrated beads hereinafter) and (b) beads that have been equilibrated with ethanol (ethanol-equilibrated beads hereinafter) redispersed in water. It will show that the time dependency of the dielectric behaviors directly reflects these non-equilibrium processes such as ion diffusion process, solvent diffusion process and solvent uptake process.

2. Experimental and methods

2.1. Dried beads in Cl-form

The IER beads used here are D_{301} macroporous anion-exchange resin beads commercially available from ZhengGuang Resin Ltd. in HangZhou China, which corresponds to Amberlite IRA-93 in U.S.A. The beads are 0.28–0.45 mm in diameter and contacting *tert*-ammonium group to matrix of styrene-divinylbenzene copolymer. The beads were transformed by saturated NaCl solution by allowing them to be dispersed in saturated NaCl solution for at least 48 h. Then they were washed by distilled water several times until the conductivities of the supernate were reduced to the values of distilled water. Finally, the sediments of the beads were collected to dry in vacuum dryer for about 8 h.

2.2. Preparation of suspensions

2.2.1. Beads in primary alcohols and water–ethanol mixtures

Before dielectric measurement, copies of dried beads of equal weight were, respectively, immersed in 50 mL primary alcohols, including methanol, ethanol, *n*-propanol, *n*-butanol, *n*-pentanol and *n*-hexanol, and water–ethanol mixtures for 48 h. The volume fractions of ethanol in the mixtures were ranging from 0 to 100%, with 20% intervals. When in dielectric measurement the dielectric cell was charged with slurry of the beads with the electrodes being totally submerged by the slurry. The slurry in fact was densely packed sediments of the resin beads in solution. The supernates (see Fig. 1) are measured independently to obtain the values of dispersion medium's dielectric constant ε_a and conductivity κ_a.

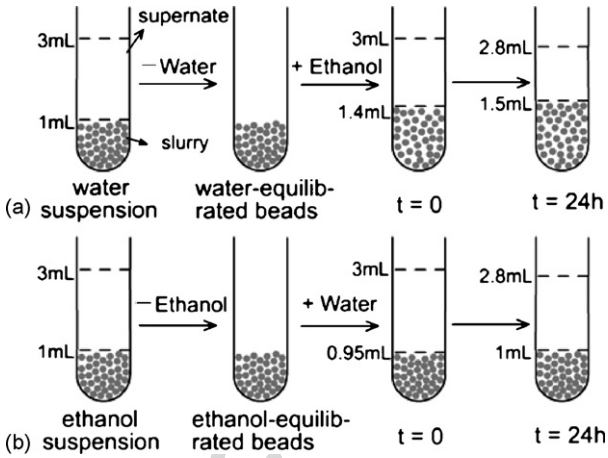

Fig. 1. The preparation process of the suspensions of water-equilibrated beads redispersed in ethanol (a) and ethanol-equilibrated beads redispersed in water (b).

2.2.2. Water-equilibrated beads in ethanol and ethanol-equilibrated beads in water

Fig. 1 shows the preparation process of the suspensions. After IER beads had been equilibrated with water, 3 mL admixture was taken into the dielectric cell with 1 mL slurry. Then all the bulk water was extracted by a microinjector and only bare water-equilibrated beads were left. After that, ethanol was quickly added into the cell until the volume of the admixture reached 3 mL. This time was taken to be zero ($t = 0$), and dielectric measurement on slurry started then. The dielectric behavior was recorded every 100 s during 0–30 min, every 10 min during 30 min–2.5 h and every 1 h during 3–24 h. It was observed that when ethanol was added, the volume of slurry increased to 1.4 mL at $t = 0$ and 1.5 mL at $t = 24$ h, while the whole volume reduced to 2.8 mL at $t = 24$ h, as shown in Fig. 1(a). Similar preparation was done to the suspension of ethanol-equilibrated beads redispersed in water as shown in Fig. 1(b).

2.3. Dielectric measurement

Dielectric measurements were carried out with a precise impedance analyzer Agilent 4294A from Agilent Technologies at frequency ranging between 40 Hz and 110 MHz. The dielectric cell used in our study consists of concentrically cylindrical platinum electrodes [28], and the cell constant and stray capacitance that have been determined by use of several standard liquids were 0.67 and 0.12 pF, respectively. The experiments were carried out at $30 \pm 0.5\,^{\circ}C$ and all experimental data were

subjected to certain corrections [29] for the errors arising from residual inductance due to the cell assembly.

2.4. Determination of relaxation parameters from experimental spectra

The dielectric relaxation parameters were obtained by fitting the following equation, which includes one ($i=1$) or two ($i=1$, 2) Cole–Cole's terms [30] and an additional term considering the electrode polarization [22], to the experimental dielectric spectra:

$$\varepsilon^* = \varepsilon - \frac{j(\kappa-\kappa_1)}{\omega\varepsilon_0} + A\omega^{-m} = \varepsilon_h + \sum_i \frac{\varepsilon_1-\varepsilon_h}{1+(j\omega\tau_i)^{\beta_i}} + A\omega^{-m} \quad (1)$$

where $\varepsilon^* = \varepsilon' - j\varepsilon''$ is complex permittivity, ε dielectric constant, κ electrical conductivity, ω angular frequency, ε_0 the permittivity of vacuum, β the Cole–Cole parameter ($0<\beta\leq 1$) and $j^2=-1$. $\tau(=1/(2\pi f_0))$ is characteristic relaxation time, where f_0 is characteristic relaxation frequency. The subscripts 1 and h denote the low and high frequency limit value, respectively, and A and m in the electrode polarization term are adjustable parameters. During the curve-fitting, the Levenberg–Marquardt method was used to minimize the sum of the residuals for the dielectric constant and electrical conductivity [22].

$$\chi = \sum_i [\varepsilon_e(\omega_i)-\varepsilon_t(\omega_i)]^2 + \sum_i [\kappa_e(\omega_i)-\kappa_t(\omega_i)]^2 \quad (2)$$

where the subscripts e and t, respectively refer to the experimental and theoretical values, and ω_i is ith angular frequency.

2.5. Dielectric analysis for IER bead suspensions

While relaxation parameters represent the collective properties of a suspension, phase parameters represent the individual electrical properties of constituent phases. According to Hanai et al. [31–33], phase parameters can be calculated in principle from relaxation parameters in light of Wagner's equation [2] (for dilute suspension) or Hanai's equation [31] (for concentrated suspension). The IER bead suspensions under research are concentrated suspensions as shown in Fig. 1, and thereby their M–W dielectric relaxation can be excellently simulated by Hanai's equation:

$$\frac{\varepsilon^*-\varepsilon_i^*}{\varepsilon_a^*-\varepsilon_i^*}\left(\frac{\varepsilon_a^*}{\varepsilon^*}\right)^{1/3} = 1-\phi \quad (3)$$

where ϕ is the volume fraction of the disperse phase, and the subscripts a and i denote the continuous medium and the dispersed particles, respectively. The phase parameters (ϕ, ε_i, κ_i and κ_a) thus are approximately related to the relaxation parameters (ε_1, ε_h, κ_1 and κ_h) as [22,33]:

$$\frac{\varepsilon_h-\varepsilon_i}{\varepsilon_a-\varepsilon_i}\left(\frac{\varepsilon_a}{\varepsilon_h}\right)^{1/3} = 1-\phi \quad (4)$$

$$\varepsilon_1\left(\frac{3}{\kappa_1-\kappa_i}-\frac{1}{\kappa_1}\right) = 3\left(\frac{\varepsilon_a-\varepsilon_i}{\kappa_a-\kappa_i}+\frac{\varepsilon_i}{\kappa_1-\kappa_i}\right)-\frac{\varepsilon_a}{\kappa_a} \quad (5)$$

$$\kappa_h\left(\frac{3}{\varepsilon_h-\varepsilon_i}-\frac{1}{\varepsilon_h}\right) = 3\left(\frac{\kappa_a-\kappa_1}{\varepsilon_a-\varepsilon_i}+\frac{\kappa_1}{\varepsilon_h-\varepsilon_i}\right)-\frac{\kappa_a}{\varepsilon_a} \quad (6)$$

$$\frac{\kappa_1-\kappa_i}{\kappa_a-\kappa_i}\left(\frac{\kappa_a}{\kappa_1}\right)^{1/3} = 1-\phi \quad (7)$$

Since the values of ε_a and κ_a can be obtained by directly measuring the supernate, the phase parameters can be determined from the relaxation parameters by using Eqs. (4)–(7), and the value of κ_h, which is generally hard to be determined by fitting dielectric spectra, can be also determined.

3. Results and discussion

3.1. IER beads suspensions in primary alcohols

Fig. 2 shows the dielectric spectra of IER beads suspensions dispersed in 1–6 primary alcohols, where $\varepsilon''=(\kappa-\kappa_1)/\omega\varepsilon_0$ is imaginary part of complex permittivity or dielectric loss. Marked dielectric relaxations with characteristic relaxation frequencies ranging from 10^4 to 10^7 Hz are shown in the spectra.

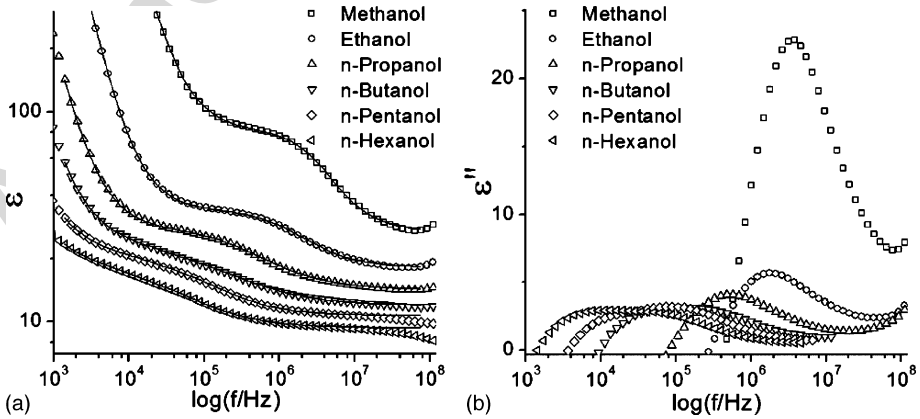

Fig. 2. Frequency dependences of the dielectric constant (a) and dielectric loss (b) of the IER beads suspensions in different primary alcohols. The solid lines are the best fit curves calculated from Eq. (1).

Table 1
Relaxation parameters and phase parameters for suspensions of IER beads dispersed in primary alcohols

Suspension	ε_l (ε_{l1})	ε_h (ε_{l2})	ε_h (ε_{h2})	κ_l (κ_{l1}) (mS/m)	κ_{h1} (κ_{l2}) (mS/m)	κ_h (κ_{h2}) (mS/m)	τ_1 (ns)	τ_2 (ns)	ε_a	κ_a (mS/m)	ε_i	κ_i (mS/m)	ϕ
Methanol	82.7		26.9	9.11		21.3		45	32.5	2.12	22.3	34.0	0.52
Ethanol	33.9		17.6	2.06		3.77		98	24.6	0.924	10.0	6.14	0.40
n-Propanol	28.4		14.2	0.471		0.960		384	20.6	0.231	5.73	1.56	0.36
n-Butanol	24.0	22.0	11.9	0.210	0.213	0.351	6356	761	17.4	0.115	4.10	0.655	0.33
n-Pentanol	22.3	18.7	10.7	0.0800	0.0824	0.152	13645	1355	14.7	0.0450	4.01	0.262	0.31
n-Hexanol	20.7	17.8	9.38	0.0400	0.0409	0.0724	28177	3105	12.7	0.0211	3.80	0.153	0.31

Note: The subscripts 1 and 2 denote lower- and higher-frequency relaxation term, respectively. The values of ε_a and κ_a were obtained by directly measuring the supernates.

These relaxations are of M–W type because counterion polarization relaxation contribution falls outside the frequency window investigated due to the beads' large radius [25]. From Fig. 2(b) it is clear to find that suspensions in methanol, ethanol and *n*-propanol exhibit only one relaxation while the remainders exhibit two partially overlapping relaxations.

The configuration of macroporous IER bead is pretty well understood nowadays [34,35]. Simply speaking, a dried bead is a combination of copolymer matrix and air-filled pores that have a broad size distribution ranging from a few angstroms up to several thousands of angstroms in radius [35,36]. Beads swell when dispersed in a solvent, including two separate processes, namely, filling of pores by the solvent and solvation of the copolymer matrix [35]. Accordingly when dried beads are dispersed in solvents, almost all pores can be filled by small molecule solvents, but only part of the pores (those big enough) can be filled by big molecule solvents. Considering the chainlike structure of alcohols because of hydrogen bond, methanol, ethanol and *n*-propanol are small enough to fill all pores, while the other alcohols can only partially fill the pores. It follows that three phases and hence two interfaces, say air/gel and bead/solvent, present in IER beads suspensions dispersed in *n*-butanol, *n*-pentanol and *n*-hexanol. This explains why these suspensions exhibit two relaxations [28]. Interestingly, in the recycle process when we redispersed the beads that had been equilibrated with the latter three alcohols in water, it was observed that air bubbles were adhering to the surface of each bead, obviously indicating that not all pores are filled by these alcohols.

M–W polarization in colloid suspension is ascribed to the space charge arising in the electrolyte layer adjacent to the particle surface whose thickness is of the order of the Debye length κ^{-1} [37]:

$$\kappa^{-1} = \sqrt{\frac{\varepsilon_a \varepsilon_0 KT}{e^2 \sum_i C_i Z_i^2}} \quad (8)$$

here K, T, C and Z are Boltzmann constant, absolute temperature, number concentration of free charge and valence of electrolyte solution. The time of M–W polarization thus can be estimated by

$$\tau_{MW} = \frac{\kappa^{-2}}{D} \quad (9)$$

where D is the ion diffusion coefficient. This is also approximately equal to the ratio ε_m/κ_m where the subscript m denotes the medium in which the space charge is formed. Accordingly, for suspensions in the latter three alcohols the lower frequency relaxation is associated to the air/gel interface while the higher one is associated to the bead/solvent interface.

In light of Eq. (1), the dielectric spectra for dielectric constant were curve-fitted, and the best fit curves (solid lines) are in good agreement with the experimental curves as shown in Fig. 2. The obtained relaxation parameters were listed in Table 1, from which the phase parameters concerning the properties of IER bead and bulk alcohols were determined through dielectric analysis. They were also listed in Table 1. For suspensions with two partially overlapped relaxations, $\varepsilon_{h1} = \varepsilon_{l2}$ and $\kappa_{h1} = \kappa_{l2}$ where the subscripts 1 and 2 represent lower- and higher-frequency relaxation term, respectively. Since the higher-frequency relaxation corresponds to bead/solvent interface, its relaxation parameters were used to calculate phase parameters. From Table 1 it can be seen that ε_a decreases with increasing chain length of the alcohols. Since $\varepsilon_a > 10$, analogue electrokinetic behavior to that observed in aqueous systems can be expected in these suspensions [38]. κ_a decreases with decreasing ε_a because diffusivity and concentration of simple ions like Cl^- in these alcohols decrease markedly with decreasing ε_a. Nevertheless, the ion concentration is still high enough to support an EDL similar to that formed in water [39]. The properties of EDL have important consequences for M–W polarization mechanism as shown in a number of investigations [6–12,17–24].

Fig. 3 shows the ε_a dependences of dielectric increment $\Delta\varepsilon(=\varepsilon_l - \varepsilon_h)$, conductivity increment $\Delta\kappa(=\kappa_h - \kappa_l)$ and relaxation time τ. As can be seen, with increasing ε_a the relaxation intensity, characterized by $\Delta\varepsilon$ or $\Delta\kappa$, increases while τ decreases. Since ion concentration and D markedly decrease as ε_a decreases, bead in lower dielectric constant alcohol has a thicker EDL (hence a bigger κ^{-1}) and thereby a bigger τ according to Eq. (9). Different from regular St-DVB copolymers, the IER beads under study carry fixed functional groups, and a counterion association equilibrium of the following form exists [25]:

$$\equiv[CH_2NH(CH_3)_2]^+ + Cl^- \rightarrow \equiv[CH_2NH(CH_3)_2]^+ \cdot Cl^- \quad (10)$$

where $\equiv[CH_2NH(CH_3)_2]^+$ is the fixed functional group and Cl^- is the counterion around it. The counterion association occurs through direct complexation in accordance with the present

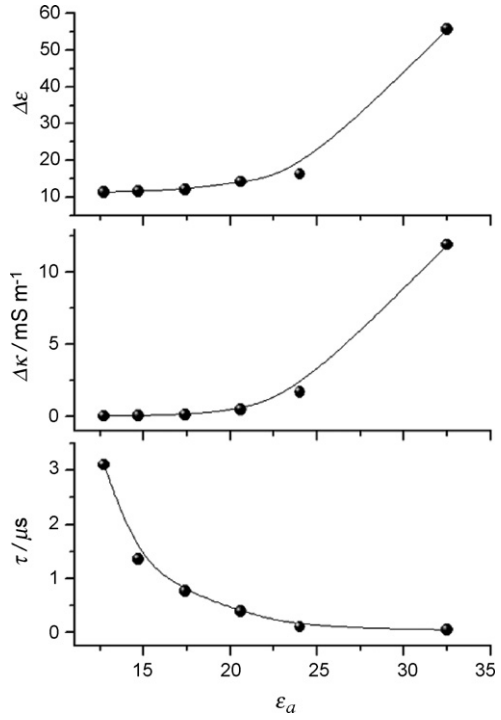

Fig. 3. Relaxation parameters for suspensions of IER beads dispersed in primary alcohols as a function of alcohols' dielectric constant. $\Delta\varepsilon(=\varepsilon_l - \varepsilon_h)$: dielectric increment; $\Delta\kappa(=\kappa_h - \kappa_l)$: conductivity increment.

understandings [40,41], analogous to weak ion-pair formation. Many factors such as counterion concentration may induce an equilibrium shift of counterion association and then change the association degree between $\equiv[CH_2NH(CH_3)_2]^+$ and Cl^-. The counterion association degree (CAD) decides how many counterions (Cl^- ion) will be left as free charges in diffuse layer and hence decides dielectric intensity for M–W dielectric relaxation as discussed in a previous work [25]. Since a high dielectric constant is in favor of having ions separated whereas a low dielectric constant will tend to have them paired [27], the CAD in alcohol with lower ε_a is higher than that with higher ε_a, leading to increasing $\Delta\varepsilon$ and $\Delta\kappa$ with increasing ε_a as seen in Fig. 3.

The properties of IER bead are changed with different alcohols as seen in Table 1, which is definitely due to the swelling process. An equilibrated bead is a combination of gel matrix and interstitial solvent (and air, for beads dispersed in the last three alcohols). And the gel matrix is an admixture of alcohol and copolymer because alcohols can swell copolymer matrix due to their lipophilic character. The ε_i thus can be approximately expressed as:

$$\varepsilon_i = f_a\varepsilon_a + f_{gel}\varepsilon_{gel} + f_{air}\varepsilon_{air} \quad (11)$$

where f is volume fraction, and $f_a + f_{gel} + f_{air} = 1$. Since ε_{gel} decreases with decreasing ε_a, ε_i evidently decreases with increasing ε_a. The values of ϕ also decrease with increasing chain length. This is probably due to the fact that a longer aliphatic group favors a better dispersion of hydrophobic copolymer particles due to the negative free enthalpy of mixing; in other words, IER beads dispersed in alcohols with longer aliphatic group are less compact than in water or alcohols with shorter aliphatic group. Fig. 1(a) shows that the volume of slurry apparently increased right after ethanol being added into the bare water-equilibrated beads. Now that ethanol uptake by the beads cannot be completed so soon, this experimental phenomenon evidently indicated that beads in ethanol, which has aliphatic group, are much less compact than in water. Therefore, the change tendency of ϕ shown in Table 1 is reasonable. The Cl-form IER beads were dried after being equilibrated with aqueous solutions, which means that hydrated counterions (mainly Cl^- ions) exist on the wall of the inside gel matrix. As the result, the concentration of free charges is bigger inside the bead than in bulk solvent and hence $\kappa_i > \kappa_a$ as seen in Table 1.

3.2. IER beads suspensions in water–ethanol mixtures

The dielectric spectra for dielectric constant and dielectric loss of IER beads suspensions in water–ethanol mixtures with different ethanol volume fractions (vol.%) are shown in Fig. 4(a) and (b). As can be seen, the suspensions undergo well marked dielectric relaxations with characteristic relaxation frequency ranging between 10^6 Hz and 10^7 Hz. With increasing vol.%, dielectric relaxations gradually shift to lower frequency region and the relaxation intensity decreases. The relaxation parameters obtained by curve-fitting as well as the phase

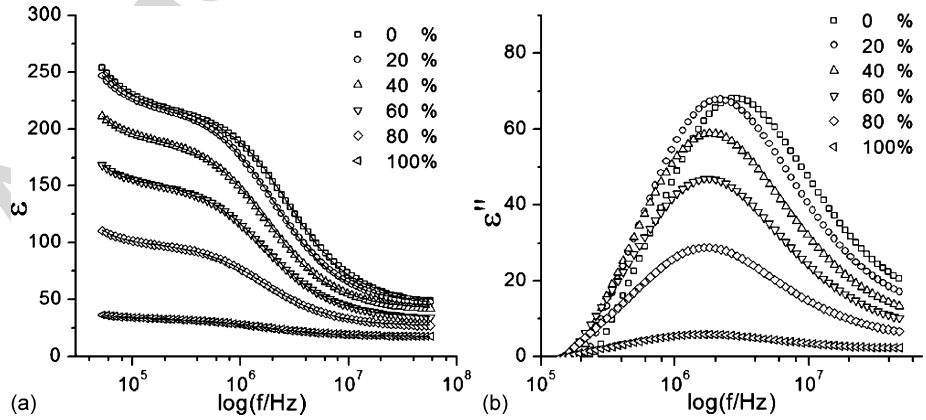

Fig. 4. Frequency dependences of the dielectric constant (a) and dielectric loss (b) of the IER beads suspensions in water–ethanol, mixtures. The solid lines are the best fit curves calculated from Eq. (1).

Table 2
Relaxation parameters and phase parameters for suspensions of IER beads dispersed in ethanol–water mixtures

Vol.%	ε_l	ε_h	$\Delta\varepsilon$	κ_l (mS/m)	κ_h (mS/m)	$\Delta\kappa$ (mS/m)	τ (ns)	ε_a	κ_a (mS/m)	ε_i	κ_i (mS/m)	ϕ
0	219.5	47.8	171.7	15.8	50.0	34.2	56.9	76.2	3.45	27.1	72.1	0.51
20	223.2	45.4	177.8	11.1	36.1	25.0	76.0	67.5	2.14	29.4	54.0	0.52
40	194.6	41.3	153.3	8.06	24.0	15.9	88.3	57.3	1.46	30.2	35.9	0.54
60	154.5	33.9	120.6	6.42	23.2	16.6	91.8	45.3	1.30	24.2	38.0	0.49
80	100.9	26.4	74.5	4.80	13.9	9.20	92.9	34.4	1.06	19.7	23.2	0.50
100	33.9	17.6	16.3	2.06	3.77	1.71	97.7	24.6	0.924	10.0	6.14	0.40

Note: The values of ε_a and κ_a were obtained by directly measuring the supernates.

parameters determined through dielectric analysis are listed in Table 2.

The directly measured values of ε_a and κ_a decrease as vol.% increases, which means that with increasing ethanol content κ^{-1} and the CAD increase. Accordingly τ increases while $\Delta\varepsilon$ and $\Delta\kappa$ decrease as vol.% increases, basically coinciding with the conclusion in the preceding section. However, it is noticeable that, when vol.% increased from 0 to 20% $\Delta\varepsilon$ is barely changed even though τ changes obviously, signifying that $\Delta\varepsilon$ can hardly be influenced by the added ethanol when vol.% $\leq$ 20%. This is possibly due to the molecular structure of water–ethanol mixtures. About the structure, microwave dielectric analysis [42] demonstrated that cluster of pure water only appears when $x_w > 0.83$ for water–alcohol mixtures, where x_w is the mole fraction of water; and adiabatic compressibility investigation [43] indicated that ethanol molecules are essentially dispersed and surrounded by water molecules at low ethanol concentration. When vol.% $\leq$ 20% (correspondingly $x_w \geq 0.928$), ethanol molecules are believed completely hydrated and cluster of pure water is the main structure form in these mixtures, therefore suspensions in these mixtures have equivalent CAD as compared with those in pure water, leading to a comparable $\Delta\varepsilon$.

It is reported [44,45] that when porous St-DVB copolymer bead is dispersed in water, water is just accommodated in the already existing air-filled pores and cannot swell the copolymer matrix, while ethanol can both fill the pores and swell the matrix. Therefore, IER beads dispersed in ethanol–water mixture are somewhat "fatter" than in pure water, and their properties and dispersing state will change in principle with the constitution of ethanol–water mixtures. Fig. 5 shows the phase parameters as a function of ethanol's volume fraction. As can be seen, κ_i and κ_a basically decrease as vol.% increases and $\kappa_i > \kappa_a$, this is mainly because of the same reason discussed in the preceding section. However, ε_i increases before the point vol.% = 40% while decreases after that with increasing vol.%. This is definitely due to the swelling process: according to Eq. (11) (the added term of air in the pores no longer exist here), when vol.% < 40%, although ε_a and f_a decrease with increasing vol.%, ε_{gel} and f_{gel} increase because of ethanol uptake, the net result is that ε_i increases with increasing vol.%; when vol.% > 40%, the amount of ethanol in bulk solvent may has exceeded what the gel matrix can absorb so that ε_{gel} no longer increases, while ε_a keeps decreasing, consequently ε_i decreases with increasing vol.%. A similar result can be observed with reference to ϕ: the highest value of which also shows up when vol.% = 40%. Although ϕ decreases with increasing ε_a as aforementioned, ethanol uptake of the gel matrix can, to some extent, increase the size of the beads, therefore ϕ increases until the gel matrix is no longer able to absorb ethanol, say when vol.% > 40%.

3.3. Suspensions of water-equilibrated beads redispersed in ethanol and ethanol-equilibrated beads redispersed in water

The dielectric behaviors of the above suspensions were measured in their equilibrium state, so the properties of these systems did not change with time during measurement. In what follows, the suspensions under study are in non-equilibrium state; nevertheless it is believed that these non-equilibrium processes can be detected by DRS. Fig. 6 gives us the three-dimensional representations of time dependency of dielectric constant spectrum for suspensions of water-equilibrated beads redispersed in ethanol (a) and ethanol-equilibrated beads redispersed in water (b). As can be seen, both suspensions display apparent time dependences with distinct M–W dielectric relaxations. Since ε_a and κ_a change with time, the phase parameters cannot be determined

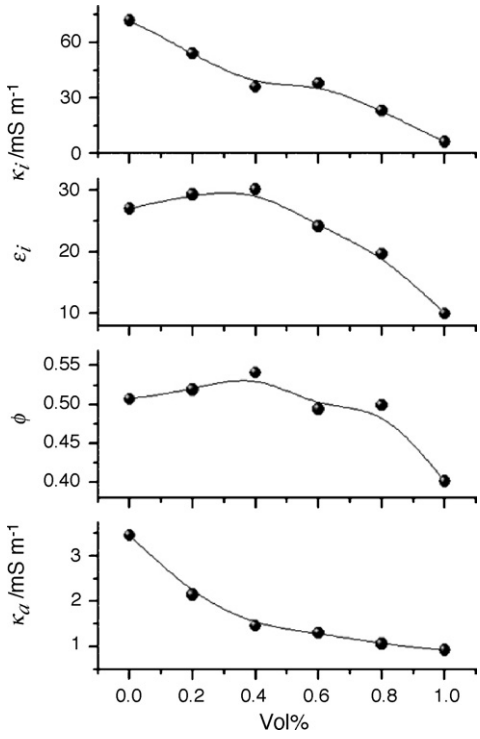

Fig. 5. Phase parameters for suspensions of IER beads dispersed in ethanol–water mixtures as a function of ethanol's volume fraction.

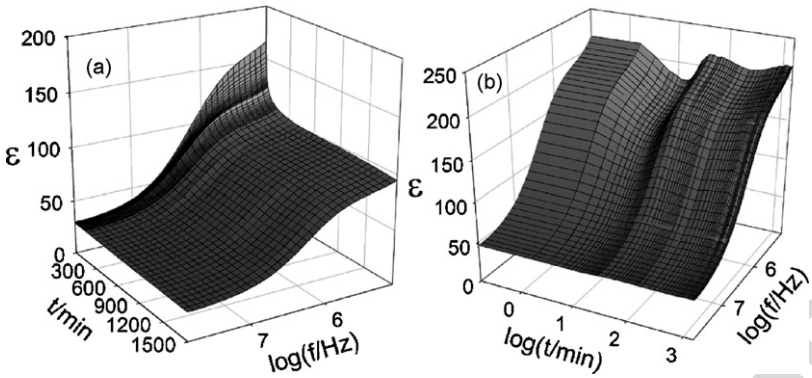

Fig. 6. Three-dimensional representations of time dependency of dielectric constant spectrum for suspensions of (a) water-equilibrated beads redispersed in ethanol and (b) ethanol-equilibrated beads redispersed in water.

in line with Eqs. (4)–(7), and only relaxation parameters will be discussed in this section.

Fig. 7 shows the variation of dielectric relaxation parameters for suspension of water-equilibrated IER beads redispersed in ethanol as a function of time. It is noteworthy that an obvious transition shows up in each curve at $t \approx 100$ min, before which the parameters change intensely with time while after which they are almost held fixed. This seems to imply that equilibrium was reached within 100 min for the present case. As discussed above, τ is mainly a function of κ^{-1} and D, and $\Delta\varepsilon$ is basically decided by CAD. The Cole–Cole parameter β represents relaxation time distribution: the bigger the value of β is the fewer mechanisms are implicated. The values of β are ranging between 0.80 and 0.84, definitely indicating that the dielectric relaxations are mainly attributed to one mechanism, namely M–W polarization. The variation of these parameters with time is believed to arise from the non-equilibrated processes that the suspension was undergoing. These processes are mainly as follows: (1) ethanol uptake by the gel matrix; (2) diffusion of bulk ethanol to water inside beads; and (3) diffusion of inside water to bulk ethanol. They should occur simultaneously, but may be completed at different moment.

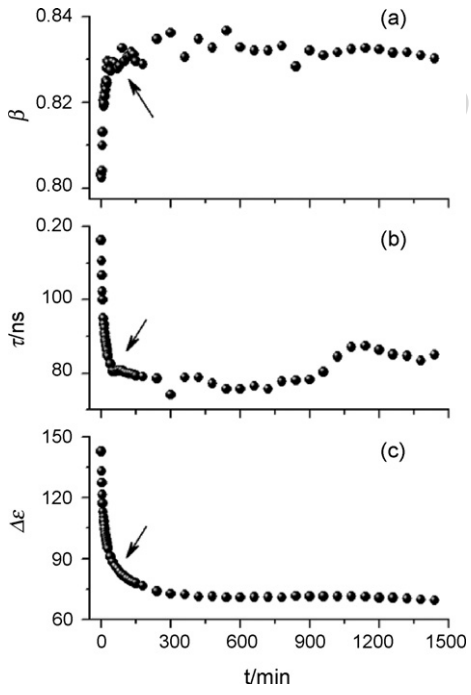

Fig. 7. Relaxation parameters for suspensions of water-equilibrated beads redispersed in ethanol as a function of time. The arrows are drawn for guiding eyes.

At $t = 0$, κ^{-1} is large and D is relatively small since the dispersion medium was substituted by ethanol, accordingly τ is initially big as seen in Fig. 7. $\Delta\varepsilon$ is initially big too, this is a little surprising because the CAD should be much high when in ethanol and a small amount of free charges should exist in the interface. It should be remembered that the beads have been equilibrated with water, therefore an aqueous membrane is believed to present on their surfaces even though the bulk water has been removed. This aqueous membrane is actually the EDL formed in water, basically including a compact layer (stern layer) and a loose diffuse layer. When ethanol is added, the diffuse layer can be immediately interfered while the compact layer can barely be influenced at the very beginning. Therefore, κ^{-1} is apparently increased while the CAD varies not so distinctively, resulting in a big initial $\Delta\varepsilon$. As seen in Fig. 7(b) and (c), $\Delta\varepsilon = 142.9$ and $\tau = 116$ ns when $t = 0$, while for suspension in 40% water–ethanol mixture $\Delta\varepsilon = 153.3$ and $\tau = 88.3$ ns as Table 2 shows. The values of $\Delta\varepsilon$ are comparable while the value of τ is much bigger of the former than the latter, which signifies that the phase constitution in compact layer (water prevails) is much different from that in diffuse layer (ethanol prevails) when $t = 0$.

As time elapses the above mentioned processes are occurring, consequently ε_a and the bulk ion concentration increase with time due to process (3). At the same time, the water membrane is gradually destroyed. As a result, κ^{-1} and CAD decrease and hence τ and $\Delta\varepsilon$ decrease with time for $t < 100$ min. The present dielectric behavior is opposite to those of equilibrium suspensions for which an increasing τ always corresponds to a decreasing $\Delta\varepsilon$ as seen in Tables 1 and 2. This result implies that for suspensions in non-equilibrium state it is the properties of interface instead of those of constituent phases that count most for M–W polarization. According to Fig. 7, these processes are all completed within about 100 min, and then equilibrium is reached, so the relaxation parameters almost no longer change with time. When $t > 100$ min, it is noticed that $\Delta\varepsilon \approx 75$ and $\tau \approx 80$ ns. These values are equivalent to those of suspension in 80% water–ethanol mixture as shown in Table 2, evidently indi-

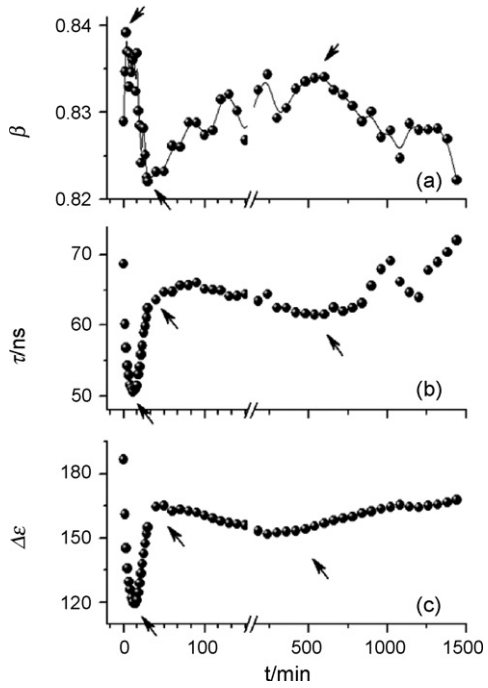

Fig. 8. Relaxation parameters for suspensions of ethanol-equilibrated beads redispersed in water as a function of time. The arrows and solid lines are drawn for guiding eyes.

cating that equilibrium has been reached. As for β, the diffusion processes definitely cause a more complicated bead/solution interface, therefore more polarization mechanisms exist in the non-equilibrium state, giving rise to an increasing β with time.

Fig. 8 shows the variation of dielectric relaxation parameters for suspension of ethanol-equilibrated IER beads redispersed in water with time, from which we can judge that more complex processes are occurring in this suspension. Three obvious transitions show up in each curve, indicating four distinct stages during the swelling process. Considering that the beads are initially ethanol-equilibrated, when they are dispersed in water the following processes are mainly about to happen: (1) diffusion of Cl^- and other simple ions from inside bead to bulk solution. Since the beads are originally ethanol equilibrated, the CAD is rather high. When water is added, the fixed functional groups as well as their counterions, both on the surfaces and inside the beads, will be directly exposed to water. As a result some counterions will be released as free ions due to the decrease of CAD, and will diffuse to bulk solution through ion-exchange; (2) diffusion of ethanol in the pores to bulk solution; (3) diffusion of bulk water to inside beads; and (4) diffusion of ethanol in the gel matrix to bulk solution. Similarly these processes occur at the same time, but they are definitely completed within different period of time judged from Fig. 8.

An ethanol membrane will also exist when bulk ethanol is removed. However, it must be almost drastically destroyed as soon as water is added, which may be due to the fact that the EDL formed in ethanol is far less compact than that in water. We justify this because $\Delta\varepsilon$ is rather big ($\Delta\varepsilon = 186.5$) and τ is small ($\tau = 68.7$ ns) at $t = 0$ as seen in Fig. 8(b) and (c), and these values are comparable to those of suspension in water–ethanol mixture with vol.% < 20%. Once the ethanol membrane is destroyed, a number of Cl^- ions will be set free due to directly exposure to water, therefore $\Delta\varepsilon$ is initially big. The first stage shown in Fig. 8, at which τ and $\Delta\varepsilon$ sharply decrease with time while β increase with time, is mainly a result of process (1) even though other processes happen at the same time. With diffusion of Cl^- ions from beads to bulk solution, the concentration of Cl^- ions in diffuse layer decreases, therefore $\Delta\varepsilon$ decreases with time; On the other hand, ion concentration in the bulk solution adjoining the EDL increase with time, giving rise to a decreasing κ^{-1} according to Eq. (9), therefore τ also decrease with time at this stage. β increases with time because the ion diffusion is less and less intense. The ion diffusion process is completed within about 17 min judged from Fig. 8.

The second stage is dominated by the process (2), which is completed within about 40 min. The diffusion of water into beads is sure to enormously increase the concentration of Cl^- ions inside the beads, however, most free Cl^- ions have to stay inside to keep neutrality because $\equiv[CH_2NH(CH_3)_2]^+$ is fixed on the gel matrix. In accordance with the principle of Donnan equilibrium, more water is needed inside the beads under this condition, which will lead to an urgent exclusion of ethanol at the same time. Therefore, the diffusion of ethanol from inside beads to bulk is comparably quick. Due to this process, the content of ethanol in bulk solution will increase with time, giving rise to a decreasing bulk Cl^- concentration and a decreasing ε_a with time. Now that the amount of ethanol is rather small as compared with that of water, ethanol content is pretty small so that most ethanol molecules are totally hydrated as discussed in Section 3.2. In this respect, a decreasing bulk Cl^- ion concentration will result in a decreasing CAD according to Eq. (10) and an increasing κ^{-1} according to Eq. (8), so both $\Delta\varepsilon$ and τ increase with time at the second stage. It is noticeable that β decrease with time at this stage. Since the diffusion of ethanol has to pass through the interface region, this result seems to imply that a complicated phase constitution can obviously influence relaxation distribution.

When the process (1) and (2) are completed, the diffusion of bulk water to inside beads continues due to Donnan equilibrium, this will cause the bulk counterion concentration to increase to some extent. Consequently τ and $\Delta\varepsilon$ decrease with time as a result of a decreasing κ^{-1} and an increasing CAD, respectively. This process is comparatively mild as shown in Fig. 8 and lasts about 500 min. The last stage corresponds to process (4), which is a long-lasting process because ethanol in the gel matrix is close solvating with the copolymer matrix. Its diffusion to bulk solution has a similar result as process (2) dose, but with much less intense of the former than the latter.

The actual swelling process is much more complicated because the above processes interact with one another during the process. Nevertheless, at one time and another certain process prevails so that the dielectric behavior of the whole suspension displays certain corresponding characteristics, and these characteristics can be detected by DRS and then be used to monitor these processes as demonstrated in this section.

4. Conclusion

Suspensions of IER beads dispersed in 1–6 primary alcohols exhibited distinct M–W type dielectric relaxations. Two partially overlapping relaxations were observed for suspensions in *n*-butanol, *n*-pentanol and *n*-hexanol, possibly because their molecules are too big to fill all the bead's pores. The phase parameters were determined by means of dielectric analysis, indicating that a smaller ε_a is in favor of a better dispersion of the beads and of a higher counterion association degree on their surfaces.

The dielectric behaviors displayed a regular dependence on the volume fraction of ethanol for IER beads suspensions dispersed in water–ethanol mixtures. Basically, $\Delta\varepsilon$ decreased while τ increased with increasing vol.%. However, suspension in water-rich mixture (vol.% < 20%) exhibited an exceptive dielectric behavior: $\Delta\varepsilon$ was nearly equal to that in pure water even though τ was much bigger. This is may be due to the fact that in water-rich mixture ethanol molecules are totally hydrated, and this kind of mixture thus behaves analogously to pure water in some ways. The phase parameters indicated that ε_i and ϕ increased with increasing vol.% for vol.% < 40% due to ethanol uptake by the gel matrix, while they decreased with increasing vol.% for vol.% > 40% as a result of decreasing ε_a.

Equilibrium was reached within about 100 min when water-equilibrated beads were redispersed in ethanol. This non-equilibrium process included three processes according to the above understandings. When ethanol-equilibrated beads were redispersed in water, more complicated processes occurred. It was concluded through analysis that, although four processes occurred simultaneously, the diffusion of counterions to bulk solution was completed within about 17 min, the diffusion of interstitial ethanol to bulk solution was completed within about 40 min, the diffusion of water to inside beads lasted about 500 min and the diffusion of the ethanol solvating with copolymer matrix to bulk solution was not completed even after 24 h.

As a conclusion, the extraordinary sensitivity as well as some other advantages of DRS has not been enough realized; more and wider applications of DRS to actual systems including those in non-equilibrium are fairly deserved to obtain information about systems in their working state.

Acknowledgement

Financial supports of this work by the National Natural Science Foundation of China (No: 20673014) are gratefully acknowledged.

References

[1] J.C. Maxwell, A Treatise on Electricity and Magnetism, third ed., Clarendon Press, Oxford, 1891.
[2] K.W. Wagner, Arch. Electrotech. 2 (1914) 371.
[3] S.S. Dukhin, Discuss. Faraday Soc. 51 (1971) 158.
[4] G. Schwarz, J. Phys. Chem. 66 (1962) 2636.
[5] J.M. Schurr, J. Phys. Chem. 68 (1964) 2407.
[6] S.S. Dukhin, V.N. Shilov, Dielectric Phenomena and the Double Layer in Disperse Systems and Polyelectrolytes, Wiley, New York, 1974.
[7] C.T. O'Konski, J. Chem. Phys. 64 (1960) 605.
[8] W.C. Chew, P.N. Sen, J. Chem. Phys. 77 (1982) 4683.
[9] R.W. O'Brien, Adv. Colloid Interface Sci. 16 (1982) 281.
[10] M. Fixman, J. Chem. Phys. 78 (1983) 1483.
[11] M. Mandel, T. Odijk, Annu. Rev. Phys. Chem. 35 (1984) 75.
[12] C. Grosse, K.R. Foster, J. Phys. Chem. 91 (1987) 3073.
[13] E.H.B. Delacey, L.R. White, J. Chem. Soc. Faraday Trans. 2 (77) (1981) 2007.
[14] C.S. Mangelsdorf, L.R. White, J. Chem. Soc. Faraday Trans. 293 (1997) 3145.
[15] J.J. López-García, J. Horno, F. González-Caballero, C. Grosse, A.V. Delgado, J. Colloid Interface Sci. 228 (2000) 95.
[16] C. Grosse, F.J. Arroyo, V.N. Shilov, A.V. Delgado, J. Colloid Interface Sci. 242 (2001) 75.
[17] T.L. Chelidze, A.I. Derevjanko, O.D. Kurilenko, Electrical Spectroscopy of Heterogeneous Systems, Naukova Dumka, Kiev, 1977 (in Russian).
[18] L.A. Rosen, D.A. Saville, Langmuir 7 (1991) 36.
[19] C. Grosse, M. Tirado, W. Pieper, R. Pottel, J. Colloid Interface Sci. 205 (1998) 26.
[20] M.L. Jiménez, F.J. Arroyo, F. Carrique, U. Kaatze, J. Phys. Chem. B. 107 (2003) 12192.
[21] M.L. Jiménez, F.J. Arroyo, F. Carrique, U. Kaatze, A.V. Delgado, J. Colloid Interface Sci. 281 (2005) 503.
[22] K. Asami, Langmuir 21 (2005) 9032.
[23] T.L. Chelidze, Y. Gueguen, Geophys. J. Int. 137 (1999) 1.
[24] T.L. Chelidze, Y. Gueguen, C. Ruffet, Geophys. J. Int. 137 (1999) 16.
[25] Z. Chen, K.S. Zhao, J. Colloid Interface Sci. 276 (2004) 85.
[26] K.S. Zhao, Z. Chen, Colloid Polym. Sci. 284 (2006) 1147.
[27] J. Hála, in: J.A. Marinsky, Y. Marcus (Eds.), Ion Exchange and Solvent Extraction, vol. 8, Marcel Dekker, New York, 1981, Chapter 5.
[28] T. Hanai, H.Z. Zhang, K. Sekine, K. Asaka, K. Asami, Ferroelectrics 86 (1988) 191.
[29] K. Asami, A. Irimajiri, T. Hanai, N. Koizumi, Bull. Inst. Chem. Res., Kyoto Univ. 51 (1973) 231.
[30] K.S. Cole, R.H. Cole, J. Chem. Phys. 9 (1941) 341.
[31] T. Hanai, Kolloidn Zh. 171 (1960) 23;
T. Hanai, Kolloidn Zh. 175 (1961) 61.
[32] T. Hanai, in: P. Sherman (Ed.), Emulsion Science, Academic, London and New York, 1968.
[33] T. Hanai, T. Imakita, N. Koizumi, Colloid Polym. Sci. 260 (1982) 1029.
[34] A. Guyot, M. Bartholin, Prog. Polym. Sci. 8 (1982) 277.
[35] O. Okay, Prog. Polym. Sci. 25 (2000) 711.
[36] H. Jacobelli, M. Bartholin, A. Guyot, Angew. Makromol. Chem. 80 (1979) 31.
[37] S.S. Dukhin, Adv. Colloid Interface Sci. 61 (1995) 17.
[38] Ph.C. Van der Hoeven, J. Lyklema, Adv. Colloid Interface Sci. 42 (1992) 205.
[39] M. Kosmulski, Colloid Surf. A 95 (1995) 81.
[40] D.E. Yates, S. Levine, T.W. Healy, J. Chem. Soc. Faraday Trans. I. 70 (1974) 1807.
[41] N. Kallay, S. Zalac, J. Colloid Interface Sci. 230 (2000) 1.
[42] S. Mashimo, T. Umehara, J. Chem. Phys. 95 (1991) 6259.
[43] G. Onori, J. Chem. Phys. 89 (1988) 4325.
[44] J.R. Millar, D.G. Smith, W.E. Marr, T.R.E. Kressman, J. Chem. Soc. (1963) 218.
[45] V.A. Davankov, S.V. Rogozhin, M.P. Tsyurupa, in: J.A. Marinsky, Y. Marcus (Eds.), Ion Exchange and Solvent Extraction, vol. 7, Marcel Dekker, New York, 1977, Chapter 2.